

LIDAR Assisted Model Predictive Control of a Next Generation Wind Turbine for Tower Fatigue Load Reduction and Improved Speed Control

Avishek A. Kumar, Patrick J. Rainey, and Ervin A. Bossanyi

I. INTRODUCTION

The introduction of LIDAR based wind field sensing technology suitable for mounting on a turbine has prompted researchers to increase turbine controller performance beyond that provided by feedback only control. This increase in control performance translates to reduced speed variance, reduced loading and reduced actuator usage leading to reduced costs of energy. Model Predictive Control (MPC) is a candidate method to utilize future wind speed data to control for multiple control objectives[1]. The optimization can include system constraints, system nonlinearities, simultaneously control multiple actuators to achieve multiple control objectives and incorporate information about future disturbances such as that supplied by LIDAR; all of which make this control framework extremely applicable to the wind turbine application.

Recently MPC methods utilizing future disturbance information have been investigated [2]–[4], showing reductions in extreme and fatigue loading and an increase in generator speed control performance. These studies indicate promising results however they are often obtained relative to a simple baseline controller and do not test the robustness of the methods in the presence of sensor noise and delays – key concerns for commercial deployment.

In this work we present comparisons of MPC controller performance when using LIDAR feedback under realistic measurement conditions (noise and delays) and against a state-of-the-art baseline controller. Key features of this implementation are: the use of an Unscented Kalman Filter (UKF) for state estimation; short prediction horizons to reduce computational burden and loop shaping of control inputs to help tune the controller response. The performance

of controllers is tested on a high fidelity *Bladed* model of a 7MW next generation wind turbine concept with a 160m rotor diameter, used for extensive cost of energy calculations by DNVGL[5].

Simulation results demonstrate a reduction in generator speed variance; a tower fore-aft fatigue load reduction; and a pitch actuator duty reduction in above rated wind conditions when using an MPC controller with LIDAR feedback.

II. APPROACH

A. Reduced Order Linear Parameter Varying Model

The wind turbine can be described by a reduced order nonlinear model which captures the dynamics relevant to the controller behavior:

$$\ddot{\delta} = \frac{Q_A}{I_r} + \frac{Q_g}{I_g N} - \left(\frac{c_{dt}}{I_r} + \frac{c_{dt}}{I_g N^2} \right) \dot{\delta} - \left(\frac{k_{dt}}{I_r} + \frac{k_{dt}}{I_g N^2} \right) \delta \quad (1a)$$

$$\dot{\omega}_g = \frac{k_{dt}}{I_g N} \delta + \frac{c_{dt}}{I_g N} \dot{\delta} - \frac{Q_g}{I_g} \quad (1b)$$

$$\ddot{x}_T = \frac{(-c_T \dot{x}_T - k_T x_T + F_T)}{m_T} \quad (1c)$$

$$\ddot{\theta}_c = -2\xi\omega\dot{\theta}_c - \omega^2\theta_c + \omega^2\theta_{cd} \quad (1d)$$

$$\dot{Q}_g = -\frac{1}{\tau_g} Q_g + \frac{1}{\tau_g} Q_{gd} \quad (1e)$$

where the δ , ω_g , x , θ_c , and Q_g represent the system states: LSS torsional deflection, generator speed, tower top fore-aft position, collective blade pitch angle and generator torque respectively; Q_A , F_T , θ_{cd} , and Q_{gd} represent system inputs: aerodynamic torque on the rotor, thrust force on the rotor, collective pitch angle demand, and generator torque demand; I_r is the rotor inertia (referred to the LSS), I_g is the generator and drivetrain inertia (referred to the high speed shaft (HSS)), N is the gearbox ratio, c_{dt} is the LSS torsional damping constant, k_{dt} is the LSS torsional stiffness constant, c_T is the modal damping of the tower flexibility, k_T is the modal stiffness of the tower flexibility, m_T is the modal mass of the tower flexibility, ξ is the pitch actuator damping ratio, ω is the pitch actuator frequency and τ_g is the generator torque time constant.

The model can be further simplified to reduce computational burden for MPC by representing the system as a Linear

A. A. Kumar is a Control Engineer with DNV GL - Energy, Auckland, New Zealand (phone: +64-9-414-5572; fax: +64-9-414-5573; e-mail: avishek.kumar@dnvgl.com).

P. J. Rainey is the Bladed Product Manager with DNV GL - Energy, Bristol, UK (phone: +44-203-816-5529; e-mail: patrick.rainey@dnvgl.com).

E. A. Bossanyi is a Senior Principal Researcher with DNV GL - Energy, Bristol, UK (phone: +44-203-816-4270; e-mail: ervin.boassanyi@dnvgl.com).

Parameter Varying (LPV) model parameterized by only by V_e and linearizing along the steady state operating trajectory:

$$\begin{aligned} \dot{x} &= A(V_e)\Delta x + B(V_e)\Delta u \\ \Delta y &= C(V_e)\Delta x + D(V_e)\Delta u \end{aligned} \quad (2)$$

where, $u = [V_e \ \theta_{cd} \ Q_{gd}]^T$, $y = [\omega_g \ \ddot{x}_T \ \theta_c \ Q_g]^T$ and $x = [\delta \ \dot{\delta} \ \omega_g \ \theta_c \ \dot{\theta}_c \ x_T \ \dot{x}_T \ Q_g]^T$.

This model maintains a degree of the nonlinearity through parameter varying coefficients, but allows the MPC optimization to be performed using the same tools as a linear system, reducing computational burden.

B. Simulation Model

The *Bladed* model of the 7MW wind turbine includes six modes for each blade (four flapwise and two edgewise modes) and seven modes for the tower (three fore-aft, three side-side and a torsional modes). The model also includes a simulated nacelle mounted continuous wave LIDAR scanning 50 equally spaced points on the circumference of circle with radius 55m, 95m upwind of the turbine at a sample time of 20ms (1s per full scan). The LIDAR returns line-of-sight data which is processed by the controller to recreate V_e over the entire prediction horizon for use by the MPC. The reconstruction of V_e from scanned points is vulnerable to error due to: sampling a single point at a time, sampling only a portion of the rotor area, the need to estimate the transport model of sampled data from the measurement plane towards the rotor plane and the decorrelation of the wind as it moves from the measurement plane to the rotor plane. All sources of error except the decorrelation are present in this investigation.

C. Baseline Controller

The state-of-the-art classically designed baseline controller used for this investigation has been heavily optimized to achieve significant reductions in cost of energy[5]. A schematic of the complete baseline control architecture can be seen in Fig 1.

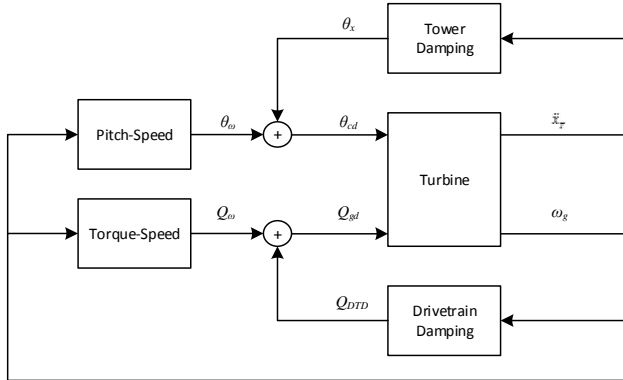


Figure 1. Schematic of baseline control architecture

D. Model Predictive Control

MPC controllers determine control inputs by optimizing a cost function of the system online. In this study an approximation of a quadratic infinite horizon cost function is used for optimizations[7]:

$$J = \sum_{i=0}^{n_p-1} \Delta x_{k+i}^T Q \Delta x_{k+i} + \Delta u_{k+i}^T R \Delta u_{k+i} + \Delta x_{k+i}^T S \Delta u_{k+i} + \Delta x_{k+n_p}^T P \Delta x_{k+n_p} \quad (3)$$

where Q is the state deviation penalty, R is the input deviation penalty, S is the cross deviation penalty and P is the terminal cost weighting. The cross term, S , allows additional tuning outputs to the control model leading to greater flexibility in loop shaping. The minimization of J can be reduced to a quadratic program (QP) by using a discrete version of (2)[2]. In the implementation used for this work we have used the ‘closed-loop paradigm’ [8] method for numerical stability and predictability.

We assume for this study that only typical, noisy turbine measurements are available to the controller, requiring state estimation. Noise and delay characteristics of the turbine IO are summarized in Table 1. (ω_g , \ddot{x}_T , θ_c and Q_g). We use a Square Root Unscented Kalman Filter (UKF) to construct state estimates from measurements[9]. The UKF is particularly suited to the turbine estimation problem as it allows for stable estimation of nonlinear systems and it provides accurate estimation of mean and covariance data for nonlinear systems in contrast to the more commonly used Extended Kalman Filter. A schematic of the complete MPC control architecture is shown in Fig. 2.

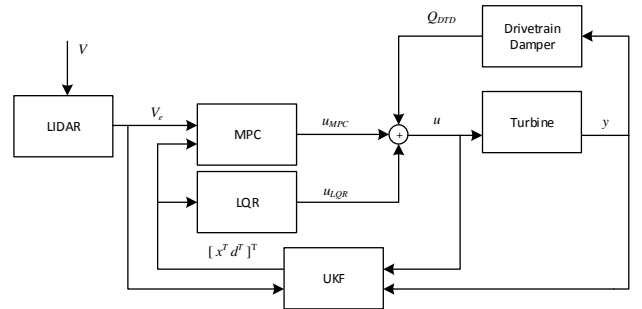


Figure 2. Schematic of MPC architecture

TABLE I. IO SIGNAL CHARACTERISTICS

Signal	ω_g	\ddot{x}_T	θ_c	Q_g	θ_{cd}	Q_{gd}
Rectangular half-width noise level	0.45 rpm	0.005 ms ⁻²	0.1°	3500 Nm	0Nm	0Nm
Delay	0.02s	0.02s	0.02s	0.02s	0.04s	0.06s

III. RESULTS

Initially four controllers have been compared in a 600s turbulent wind simulation: MPC without LIDAR based measurements (MPC); MPC with LIDAR based measurements (MPC+LIDAR); MPC with ideal V_e measurements (MPC+Ideal LIDAR) and the baseline controller. The MPC with ideal V_e allows quantification of performance loss through errors in reconstructing V_e from realistic LIDAR measurements.

The simulations have been run with 3D turbulent full field wind with a mean speed of 16ms^{-1} , created according to IEC61400-3 design standards for normal turbulence[10]. Hard constraints are placed on the inputs:

$$\begin{aligned} 0^\circ < \theta_{cd} < 90^\circ, \\ -8.5^\circ \text{ s}^{-1} < \dot{\theta}_{cd} < 8.5^\circ \text{ s}^{-1}, \\ -15^\circ \text{ s}^{-2} < \ddot{\theta}_{cd} < 15^\circ \text{ s}^{-2} \text{ and} \\ 0Nm < Q_{cd} < 195140Nm \end{aligned} \quad (4)$$

All controllers used a sample time of 0.02s and the MPC controllers used a prediction horizon of 30 steps (0.6s), just above the minimum necessary to guarantee a feasible optimization in light of the pitch input position and acceleration constraints (0.57s).

To enable a fair comparison, an MPC controller with no LIDAR input is tuned to perform as closely to the baseline as possible. The same controller was then given LIDAR based reconstructions of V_e over the entire prediction horizon (MPC+LIDAR) and perfect knowledge of V_e over the prediction horizon (MPC+Ideal LIDAR).

The results for all controllers relative to the baseline are summarized in Table 2. The MPC+Ideal LIDAR case shows the most significant performance increases with a reduction from 142% to 69% in generator speed standard deviation, a reduction from 91% to 85% in total pitch travel and a reduction from 104% to 90% in tower fatigue loading. Using LIDAR based reconstructions of V_e we see performance losses relative to the ideal case, however there is still a reduction in the generator speed variation from 142% to 74% and a tower load reduction from 104% to 94%.

As the rotor speed objective is often binary, a greater reduction in loading for the same speed control performance is preferred. In the presented paper we will include results comparing MPC controllers with LIDAR feedback detuned to have similar speed control to the baseline case to investigate the resulting load reduction.

IV. CONCLUSION

An MPC controller has been shown to reduce rotor speed variance and tower fore-aft fatigue DELs relative to a state-of-the-art feedback only baseline controller on a next generation 7MW wind turbine concept.

The investigation shows that the method is robust to practical implementation issues such as noisy and delayed IO, realistic LIDAR measurements, short prediction

horizons, reduced order LPV models and relying on state estimation.

V. LEARNING OBJECTIVES

The following learning objectives are intended for conference attendees:

- Become familiar with LIDAR technologies;
- Become familiar with MPC for wind turbines;
- Understand the practical challenges for implementing MPC for wind turbines; and
- Understand the potential benefits of adopting LIDAR assisted MPC for wind turbine control commercially.

TABLE II. CONTROLLER PERFORMANCE NORMALISED TO BASELINE

Controller	MPC	MPC + LIDAR	MPC + Ideal LIDAR
Max. Gen. Speed	104%	98%	99%
Std. Dev. Gen. Speed	142%	76%	69%
Total Pitch Travel	91%	90%	85%
Tower Base Fore-Aft DEL	104%	94%	90%

REFERENCES

- [1] D. Q. Mayne, J. B. Rawlings, C. V. Rao, and P. O. Scokaert, "Constrained model predictive control: Stability and optimality," *Automatica*, vol. 36, pp. 789–814, 2000.
- [2] A. A. Kumar, "Multivariable Control of Wind Turbines for Fatigue Load Reduction in the Presence of Nonlinearities," The University of Auckland, Auckland, 2011.
- [3] D. Schlipf, P. Grau, S. Raach, and R. Duraiski, "Comparison of linear and nonlinear model predictive control of wind turbines using LIDAR," in *Proceedings of the American Control Conference*, 2014.
- [4] M. Mirzaei and M. Soltani, "Model predictive control of wind turbines using uncertain LIDAR measurements," in *American Control Conference*, 2013.
- [5] J. Dobbin, A. Cordle, L. Blonk, D. Langston, A. Kumar, E. Bossanyi, F. Vanni, M. de Batista, O. H. Salas, and F. Davison, "Fully Integrated Design: Lifetime Cost of Energy Reduction for Offshore Wind," in *Proceedings of the Twenty-fourth (2014) International Ocean and Polar Engineering Conference*, 2014.
- [6] E. A. Bossanyi, "The Design of closed loop controllers for wind turbines," *Wind Energy*, vol. 3, no. 3, pp. 149–163, 2000.
- [7] R. Findeisen and F. Allgöwer, *{T}he quasi-infinite horizon approach to nonlinear model predictive control*. Springer, 2003.
- [8] J. A. Rossiter and H. B. Bishop, "Closed Loop Paradigm," in *Model-Based Predictive control: A Practical Approach*, Boca Raton: CRC Press, 2003, pp. 127–151.

- [9] R. Van Der Merwe and E. A. Wan, "The Square Root Unscented Kalman Filter for State and Parameter Estimation," in *IEEE International Conference on Acoustics, Speech, and Signal Processing*, 2001, pp. 3461–3464.
- [10] "IEC 61400-3: Wind Turbines-Part 1: Design Requirements." 2005.